

Effects of Image Compression on Image Age Approximation

20th International Workshop on Digital-forensics and Watermarking
Beijing, China, 20-22 November, 2021 (Online and Open)

Robert Jöch1, Andreas Uhl

Department of Computer Sciences, University of Salzburg, Austria

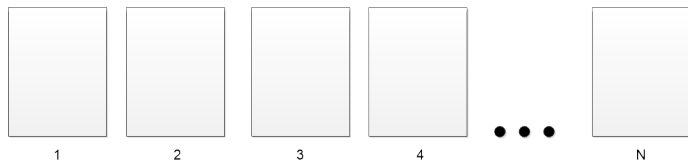
November 21, 2021



- 1 Introduction and Motivation
- 2 Age Approximation and Defect Detection Methods
- 3 Dataset and Experiments
- 4 Experimental Results
- 5 Conclusion



Trustworthy Images in Chronological Order



Approximate the Image Age **relative** to the Trustworthy Set



Untrustworthy Images

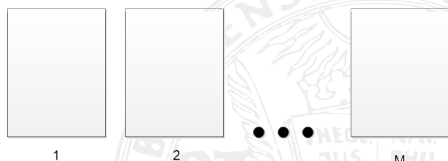


Figure: Overview image age approximation.

In-Field Sensor Defects:

- Develop after the manufacturing process and accumulate over time.
- Are due to cosmic radiation [1].
- Spread to the neighboring pixels because of preprocessing (e.g., demosaicing).

The trend towards ISO expansion and smaller pixel sizes increases the defect development rate [2].

Defect model,

$$F(I) = I + IK + \tau D + c. \quad (1)$$

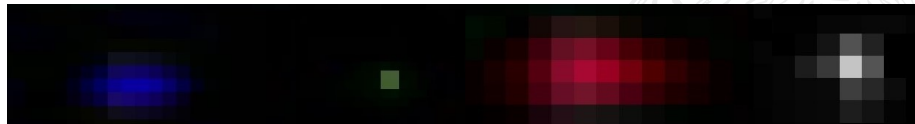


Figure: In-field sensor defects extracted from captured dark-field images.

- In-field sensor defects appear as point like spiky shot noise and noise is among high-frequency (high-detailed) image content.
- Image compression techniques usually progressively suppress high-frequency image content.

⇒ It is important to evaluate how the available defect based image age approximation methods are affected by image compression!

We assess the robustness with respect to:

- JPEG (JPG)
- JPEG 2000 (JP2)
- JPEG-XR (JXR)
- Better Portable Graphics (BPG)



In [3], Fridrich et al. propose a

Maximum Likelihood Technique (KDC).

KDC - Age Approximation Classifier

$$\hat{y} = \operatorname{argmax}_{y \in Y} \prod_{i \in \Omega} 1/\sqrt{2\pi\hat{\sigma}_{(i)}^{(y)}} \exp W_{(i)} - (l_{(i)}K_{(i)}^{(y)} + \tau D_{(i)}^{(y)} + c_{(i)}^{(y)})/2\hat{\sigma}_{(i)}^{2(y)}. \quad (2)$$

The authors assume that the difference between the median filter residual W and the sum of all defect parameter (i.e., K , D , c) is normally distributed. The proposed maximum likelihood approach 'KDC' is formalized as a classifier in equation (2).

In [4], we propose to utilize traditional machine learning techniques i.e.

Naive Bayes Classifier (NB)

Support Vector Machine (SVM)

NB - Age Approximation Classifier

$$\hat{y} = \operatorname{argmax}_{y \in Y} P(y|\vec{x}) = \operatorname{argmax}_{y \in Y} P(y) \prod_{i \in \Omega} P(\vec{x}_{(i)}|y). \quad (3)$$

The best results were achieved when $P(\vec{x}_{(i)}|y)$ is estimated with a 'Kernel Density Estimation' (NB-KDE).

In [4], we propose to utilize traditional machine learning techniques i.e.

Naive Bayes Classifier (NB)

Support Vector Machine (SVM)

SVM - Age Approximation Classifier

- The feature space is interpreted as Ω dimensional hypercube with an edge length of 511 (i.e. $[-256, 256]$).
- Find k mutually exclusive subspaces (one for each class).
- In a one vs. one scenario $\frac{k(k-1)}{2}$ SVMs are trained.
- We used the standard Matlab SVM implementation.

- Fridrich et al. suggest to threshold the median filter residual in [3]
- Since the median filter completely smooths out a peak in a homogeneous area, the method can be considered as 'spatial only' detection

Spatial only Detection

A pixel is regarded as a defect candidate if the inequality

$$\sigma^2(\vec{r}_2) > t, \quad (3)$$

$$\text{where } t = \mu + \sigma * w$$

holds. The global threshold t is defined by the average residual variance μ , the residual variance standard deviation σ and an adaptive weight $w \in \mathbb{R}^+$. The mean and standard deviation are computed over all pixels.

- We introduced a defect detection method exploiting spatial and temporal informations ('spatial & temp.') in [5].

Spatial Detection with Temporal Information

A pixel is considered defective if,

$$\sigma^2(\vec{r}_1) < \sigma^2(\vec{r}_2) \wedge \|\vec{r}'_2\|_1 > \alpha * |R_2|, \quad (4)$$

where $\vec{r}'_2(i) = \begin{cases} \vec{r}_2(i) = 0, & \text{if } t_l < \vec{r}_2(i) < t_u \\ \vec{r}_2(i) = 1, & \text{otherwise,} \end{cases}$

and $t_{l,u} = \lceil \text{median}(\vec{r}_1) \rceil \mp w_S * \sigma(\vec{r}_1)$.

The parameter α controls the amount of residual values in \vec{r}_2 that have to be outside of $[t_l, t_u]$

We rely on images from two different devices:

- Pentax K5 (P1), 4725 images (captured between 2013 and 2021).
- Pentax K5II (P2), 1881 images (captured between 2014 and 2021).

Two subsets (S_1 and S_2) are used,

- S_1 contain the first 140 available images (no regarded defects is already present).
- S_2 contain the last 140 available images (all regarded defects are already present).



Figure: Scenes Samples P1.

We rely on images from two different devices:

- Pentax K5 (P1), 4725 images (captured between 2013 and 2021).
- Pentax K5II (P2), 1881 images (captured between 2014 and 2021).

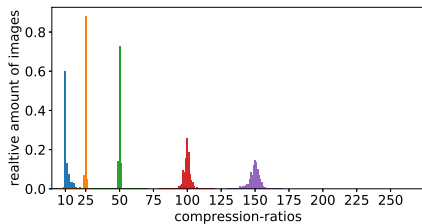
Two subsets (S_1 and S_2) are used,

- S_1 contain the first 140 available images (no regarded defects is already present).
- S_2 contain the last 140 available images (all regarded defects are already present).

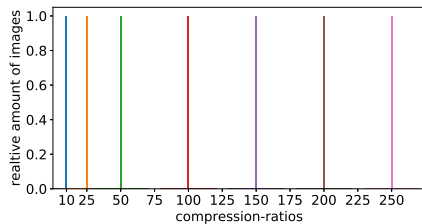


Figure: Scenes Samples P2.

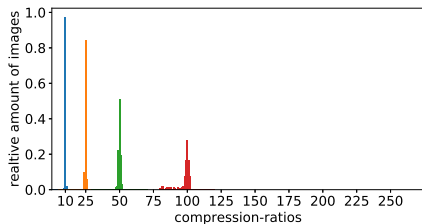
Dataset



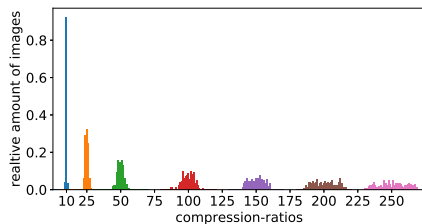
(a) JPG



(b) JP2



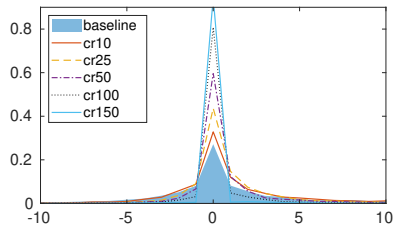
(c) JXR



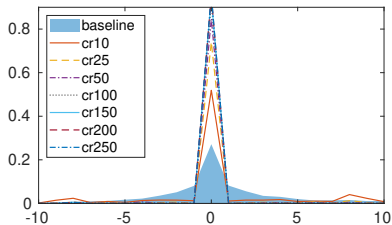
(d) BPG

Figure: Distribution of file sizes per target compression ratio and technique.

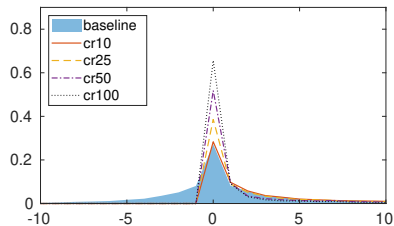
Median Filter Residual Distribution



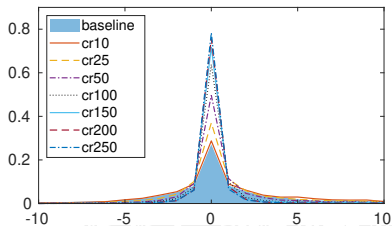
(a) JPG



(b) JP2



(c) JXR

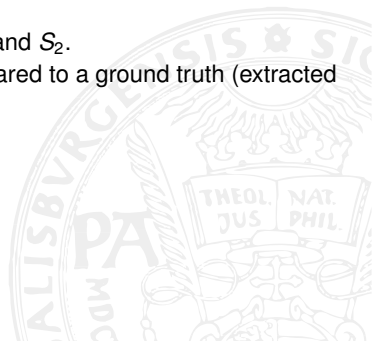


(d) BPG

Figure: Distribution of median filter residuals of defective pixels.

Evaluation of the considered defect detection methods:

- The same experiments are performed as in [5], i.e.,
 - The f1 score is computed for a broad range of parameter combinations.
 - This evaluation is performed 10 times for each compression technique and ratio.
 - 100 images are randomly drawn from S_1 and S_2 .
 - The resulting defect candidates are compared to a ground truth (extracted from dark-field images).

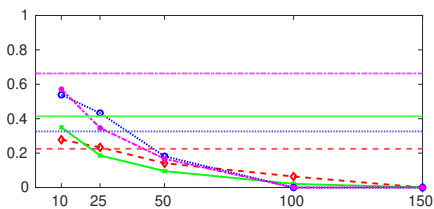


Evaluation of the considered age approximation methods:

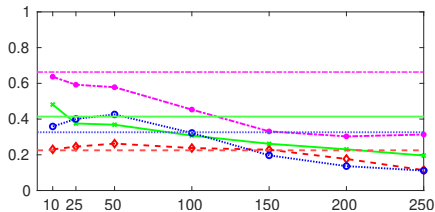
- The same experiments are performed as in [5], i.e.,
 - Image age prediction between S_1 and S_2 (binary classification problem)
 - The resulting defect candidates (True Positives and False Positives), found during the detection method evaluation (where the f1 score was maximum) are used.
 - ⇒ Based on the 10 different runs, 10 different sets of classification features result.
 - Each method is trained 200 times for each set of classification features.

Since the same images are used and the same evaluation is performed, the stated results in [5] act as baseline.

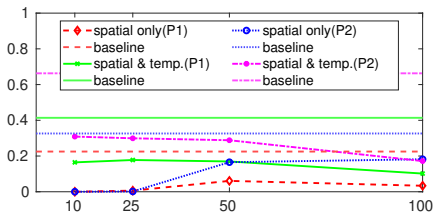
Results - Defect Detection



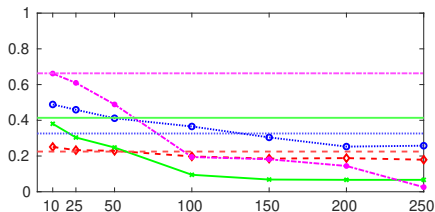
(a) JPG



(b) JP2



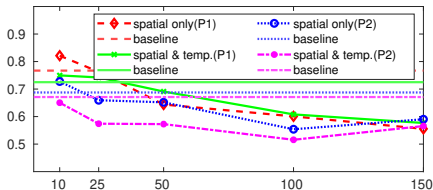
(c) JXR



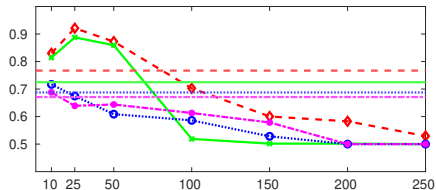
(d) BPG

Figure: Maximum average f1 score over the different target compression ratios.

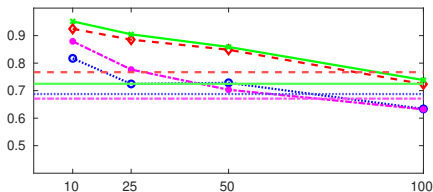
Results - Age Approximation 'KDc'



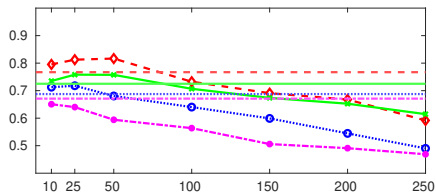
(a) KDc (JPG)



(b) KDc (JP2)



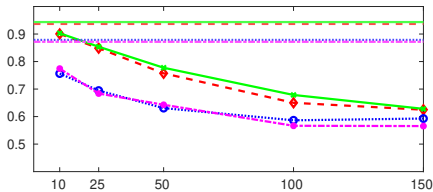
(c) KDc (JXR)



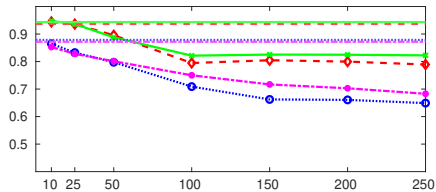
(d) KDc (BPG)

Figure: Average prediction accuracy over the different target compression ratios.

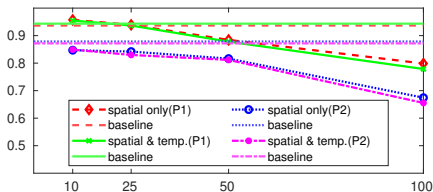
Results - Age Approximation 'NB-KDE'



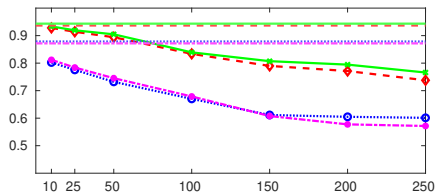
(a) NB KDE (JPG)



(b) NB KDE (JP2)



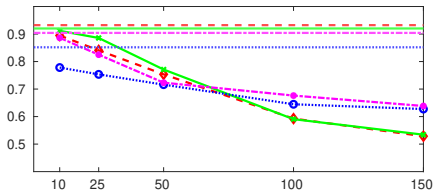
(c) NB KDE (JXR)



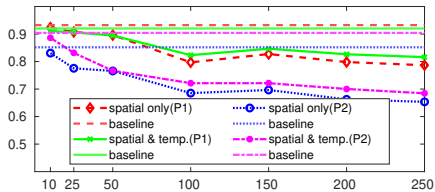
(d) NB KDE (BPG)

Figure: Average prediction accuracy over the different target compression ratios.

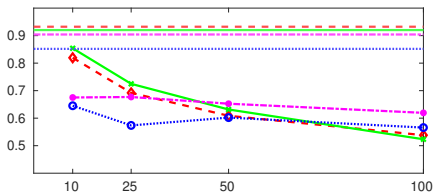
Results - Age Approximation 'SVM'



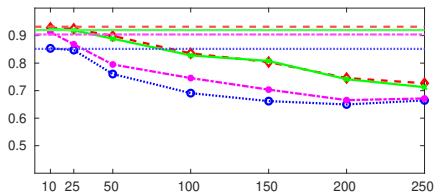
(a) SVM (JPG)



(b) SVM (JP2)



(c) SVM (JXR)



(d) SVM (BPG)

Figure: Average prediction accuracy over the different target compression ratios.

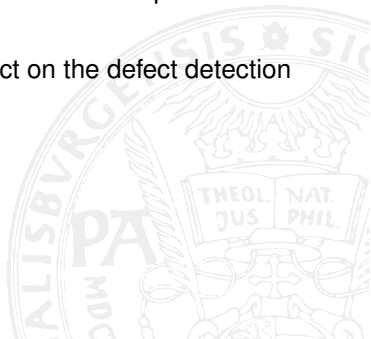
Results - Age Approximation

		JPG	JP2	JXR	BPG	$\Sigma/4$	
R_1	KDC	spatial only	0.7072	0.8317	0.8455	0.7893	0.7934
		spatial & temp.	0.6977	0.7701	0.8635	0.7393	0.7677
	NB KDE	spatial only	0.7890	0.8926	0.8949	0.8925	0.8673
		spatial & temp.	0.8032	0.8983	0.8870	0.8991	0.8719
	SVM	spatial only	0.7704	0.8809	0.6646	0.8969	0.8032
		spatial & temp.	0.7897	0.8838	0.6834	0.8903	0.8118
$\Sigma/6$		0.7595	0.8596	0.8065	0.8512		
R_2	KDC	spatial only	0.6482	0.6467	0.7259	0.6878	0.6772
		spatial & temp.	0.5782	0.6460	0.7478	0.6122	0.6461
	NB KDE	spatial only	0.6671	0.8009	0.7950	0.7451	0.7520
		spatial & temp.	0.6669	0.8080	0.7865	0.7550	0.7541
	SVM	spatial only	0.7231	0.7643	0.5967	0.7881	0.7181
		spatial & temp.	0.7777	0.8015	0.6560	0.8304	0.7664
$\Sigma/6$		0.6769	0.7446	0.7180	0.7364		

Table: Arithmetic mean of the average age prediction accuracy achieved for the first four compression ratios evaluated (i.e., compression ratio 10 - 100).

Defect detectio methods:

- The 'spatial & temp.' is superior to the 'spatial only' method at lower compression ratios.
- The 'spatial only' method tend to be more robust with respect to 'JPG' and 'BPG' compressed images.
- Overall, 'JP2' and 'BPG' show the least effect on the defect detection performance.



Age approximation methods:

- The 'KDC' classifier seems to benefit considerably from 'JXR' image compression.
- The 'NB-KDE' classifier showed the best results on 'JP2' compressed images (average accuracy up to 0.8224 for a compression ratio of 250).
- The 'SVM' classifier again showed the best results on 'JP2' compressed images.
- Overall, the most robust classifier is the 'NB-KDE' and 'JP2' the technique showing the least impact.

The most commonly used compression technique ('JPG') significantly attenuates the defect for higher compression ratios, so that defects can no longer be detected and the prediction accuracy also decreases considerably.

- [1] A. J. Theuwissen, “Influence of terrestrial cosmic rays on the reliability of ccd image sensors part 1: Experiments at room temperature,” *IEEE Transactions on Electron Devices*, vol. 54, no. 12, pp. 3260—3266, 2007.
- [2] G. H. Chapman, R. Thomas, R. Thomas, K. J. Coelho, S. Meneses, T. Q. Yang, I. Koren, and Z. Koren, “Increases in hot pixel development rates for small digital pixel sizes,” *Electronic Imaging*, vol. 2016, no. 12, pp. 1—6, 2016.
- [3] J. Fridrich and M. Goljan, “Determining approximate age of digital images using sensor defects,” in *Media Watermarking, Security, and Forensics III* (N. D. Memon, J. Dittmann, A. M. Alattar, and E. J. Delp, III, eds.), vol. 7880, pp. 49—59, International Society for Optics and Photonics, SPIE, 2011.

- [4] R. Joechl and A. Uhl, “A machine learning approach to approximate the age of a digital image,” in *Digital Forensics and Watermarking: 19th International Workshop, IWDW 2020, Melbourne, VIC, Australia, November 25–27, 2020, Revised Selected Papers*, vol. 12617 of *Springer LNCS*, pp. 181–195, Springer International Publishing, 2021.
- [5] R. Joechl and A. Uhl, “Identification of in-field sensor defects in the context of image age approximation,” in *2021 IEEE International Conference on Image Processing (ICIP)*, (Anchorage, AK, USA), pp. 3043–3047, 2021.

Thank you for your attention!

